Taylor & Francis
Taylor & Francis Group

Check for updates

Effect of Operational Conditions on Separation of Lithium from Geothermal Water by λ-MnO$_2$ Using Ion Exchange–Membrane Filtration Hybrid Process

Yaşar K. Recepoğlu[a,b], Nalan Kabay[a], Kazuharu Yoshizuka[c], Syouhei Nishihama[c], İdil Yılmaz-Ipek[a], Müşerref Arda[d], and Mithat Yüksel[a]

[a]Faculty of Engineering, Chemical Engineering Department, Ege University, Izmir, Turkey; [b]Faculty of Engineering, Department of Chemical Engineering, Izmir Institute of Technology, Izmir, Turkey; [c]Faculty of Environmental Engineering, Department of Chemical Engineering, The University of Kitakyushu, Kitakyushu Japan; [d]Faculty of Science, Chemistry Department, Ege University, Izmir, Turkey

ABSTRACT

A hybrid system coupling ion exchange and ultrafiltration (UF) was employed to separate lithium from lithium-spiked geothermal water. The effect of process parameters such as adsorbent type, adsorbent dosage, permeate flow rate, and replacement speeds of fresh and saturated adsorbents have been evaluated to determine the efficiency of the hybrid system. According to the results obtained using λ-MnO$_2$ derived from spinel-type lithium manganese dioxide, the optimal operating conditions to separate lithium from geothermal water were found with powdery λ-MnO$_2$ with an adsorbent concentration of 1.5 g adsorbent/L solution, replacement rates of fresh and saturated adsorbents of 6.0 mL/min, and a permeate flow rate of 5.0 mL/min. The ion exchange–UF hybrid system providing an advantage to work with very fine particles easily can be considered as a favorable process for the separation of lithium from geothermal water.

KEYWORDS
Geothermal water; hybrid process; lithium; ion exchange; membrane

Introduction

Along with its superior properties and broad range of application areas, lithium is taken into account as the major element of the modern life in the 21st century.[1–3] A continuous improvement in lithium ion batteries since 1990s with the vast battery applications such as electrical vehicles or stationary storage systems is the dominating issue in terms of cost and energy saving.[4]

The scarcity of lithium from mineral resources has pushed the researchers toward the utilization of liquid lithium resources such as salt lake brine, seawater, and geothermal water, which have been estimated to contain >85% of the world's recoverable lithium.[5–10] It was reported in the literature that the geothermal waters in Japan contain larger amounts of Li (approximately 10 mg/L from reaction of the geothermal water with rocks in the aquifer) than in seawater and other liquid resources.[1,6]

As summarized in Table 1, there are several separation methods such as adsorption, solvent extraction, and membrane processes to recover lithium from aqueous solutions. Among these methods, the adsorption by using λ-MnO$_2$ adsorbent is one of the most studied.[9,10,13–19]

The λ-type manganese dioxide (λ-MnO$_2$) is the most efficient lithium adsorbent because of its excellent ion-sieve property together with its host property. The memory effect of the hole formed after lithium exchange embodies these special properties of this adsorbent. It is usually comprised of


Color versions of one or more of the figures in the article can be found online at www.tandfonline.com/lsei.

Table 1. Methods for lithium separation from aqueous media.

Method	Resource	Outcomes	Drawbacks	Reference
Batch adsorption	Urmia Lake brine	The synthesized MnO_2 nanorods can be used in lithium extraction from brines, seawater, and wastewater.	Time-consuming and discontinuous operation.	[8]
Chromatographic adsorption	Geothermal water	The adsorption of Li with the λ-MnO_2 was successfully achieved in sequential column operations.	Despite continuous operation, also time consuming.	[7]
Solvent extraction	Aqueous solution	Functionalized ionic liquids can be used to broaden the potential utility of liquid–liquid extraction processes and establish efficient and environmentally friendly processes for the separation of valuable metal ions.	Limited selectivity, difficulty of automation, and emulsions.	[5]
Bipolar membrane electrodialysis	A mixed solution of lithium and cobalt	The selectivity for lithium in the recovery cell was about 99%.	The chemical stability, especially against concentrated alkaline solutions is too low.	[11]
Nanofiltration (NF) and low-pressure reverse osmosis (LPRO)	Salt lake brines	NF90 membrane was more effective for Li^+ extraction from a diluted brine due to its higher hydraulic permeability to pure water (L_p = 15 L h^{-1} m^{-2} bar^{-1}).	Chemical resistance and limited lifetime of membranes	[12]

a several spinel-type lithium manganese dioxides with a chemical formula of $Li_{1+x}Mn_{2-x}O_4$ ($0 < x < 0.33$). The molar ratio of Li/Mn differs in a relatively wide range, but $Li_4Mn_5O_{12}$ is one of the most promising adsorbents for lithium because of its large adsorption capacity, as well as high chemical stability.[18,19] The ion exchange reaction occurs only between lithium and hydrogen ions as shown in Equation 1.[20]

$$3Li_{1.33}Mn_{1.67}^{4+}O_4 + H^+ \rightarrow 3H_{1.33}Mn_{1.67}^{4+}O_4 + 4Li^+ \tag{1}$$
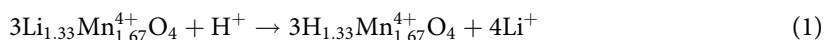
In the literature, the high selectivity of this adsorbent for lithium ions with high separation coefficients of $\alpha_{Li/Mg} = 109.5$, $\alpha_{Li/Na} = 220.7$, and $\alpha_{Li/K} = 125.5$ was reported.[21] The adsorbent λ-MnO_2 was well developed from spinel-type lithium dimanganese tetraoxide ($LiMn_2O_4$ and $Li_{1.5}Mn_2O_4$) for the selective separation of lithium from seawater.[10,13]

As we published before, the maximum lithium adsorption capacities from lithium-spiked geothermal water during batch adsorption tests were obtained as 31.55 mg/g for powdery λ-MnO_2 and 30.42 mg/g for granulated λ-MnO_2.[22] Nishihama et al.[17] reported that the separation of lithium from seawater using the column-mode operation with granulated λ-MnO_2 adsorbent exhibited around 33% of recovery for lithium. On the other hand, there should be some improvements to increase the adsorption efficiency of the fixed bed adsorption method by combining with another process. Although an ion-sieve adsorbent, λ-MnO_2 is a promising material because of its extreme selectivity toward lithium ion,[18] and its original powdery form may not work well in a fixed-bed column operation. For this reason, the membrane filtration can be integrated to the adsorption process to overcome the difficulty of separation of the powdery adsorbent particles from the solution as well as to utilize the adsorbent with a high efficiency resulting in a higher uptake and better kinetics. Moreover, synergetic effects emerging at the membrane surface may generate a high intensification of the process.[23]

The ion exchange–membrane filtration hybrid method was particularly applied for boron removal from geothermal water and seawater.[24–31] It was also applied for the removal of bisphenol A from aqueous solution.[32]

Recently, we have conducted a preliminary study for simultaneous separation of boron and lithium from geothermal water by ion exchange–membrane filtration hybrid process offering an efficient way to extract lithium from geothermal water due to usage of boron selective ion exchange resin containing N-methyl-D-glucamine (NMDG) functional group, which has affinity for arsenic.

Since λ-MnO_2 adsorbents can also show some affinity for arsenic, this affinity was suppressed by a boron-selective ion exchange resin containing the NMDG group. Separation efficiencies for lithium and boron from geothermal water were found to be 100% and 83% using boron selective ion exchange resin Dowex XUS-43594.00 and lithium selective λ-MnO_2 adsorbent simultaneously.[33]

In this study, the efficiency of λ-MnO_2 adsorbents for the separation of lithium from lithium-spiked geothermal water was studied by using hybrid process integrating ion exchange with UF. The optimum process parameters such as type and concentration of adsorbent in the suspension (C, g/L), replacement rates of fresh and saturated adsorbents (Qs, mL/min), and flow rate of permeate stream (Qp, mL/min) were determined during the operation.

Experimental

Materials

The adsorbent λ-MnO_2 with powdery and granulated forms has been synthesized by the same manner described in the literature.[9,13] The preparation procedures were as follows:

Powdery Mn_3O_4 and $LiOH \cdot H_2O$ were mixed at a 0.75 molar ratio of Li/Mn and ground for 1 h with a ball mill. The mixture was then sintered at 425°C for 5 h in an electrical oven. After cooling to room temperature, it was mixed and ground again for 1 h. The mixture was again sintered at 500°C for 5 h. After slow cooling to room temperature, powder spinel-type lithium dimanganese tetroxide ($Li_{1.5}Mn_2O_4$) having 0.01–0.05 mm particle size range was obtained as an intermediate product whose properties are given in Table 2.

Conditioning of the powdery and granulated adsorbents (5 g) was performed by treatment with 1.0 M HCl (1 L), via shaking at room temperature for 24 h. After acid treatment, the adsorbent was washed with deionized water until reaching pH 4–5 in washings. Subsequently, the adsorbents were filtered using a 0.45-μm membrane filter, air dried, and then dried in a vacuum oven until a constant weight was obtained.

The granulation of the adsorbents was carried out with alumina-based binder. The powdery λ-MnO_2 (8.0 g) and the alumina-based binder (product of CATALOID AP-1, JGC Catalysts and Chemicals Ltd., Kawasaki, Japan) (2.0 g) were mixed together with a small amount of deionized water. The kneaded mixture was pressed out from 1-mm hole in diameter by an extruder and then dried at room temperature for overnight. The mixture was calcinated at 550°C for 3 h, and then was cut into small pieces of 1 mm length.

Geothermal water samples obtained from Izmir Geothermal Co., Balçova, Turkey were used in the experimental studies. The properties of geothermal water sample employed are listed in Table 3.

For adsorption–membrane hybrid tests, geothermal water samples were spiked with standard lithium solution (LiCl) in a way that lithium concentration is around 11–12 mg/L.

The specifications of the submerged-style hollow fiber ZeeWeed®-1, Haifa, Israel (ZW-1, GE) Model UF module utilized in the adsorption–ultrafiltration (UF) hybrid process based on the catalogue are given in Table 4.

Table 2. Properties of λ-MnO_2 adsorbent.

Type	Spinel
Form	Powdery
Specific surface area, m²/g	68 m²/g
Mean particle size, mm	0.01–0.05
Total lithium capacity, mg Li/g	31.55

Table 3. Analyzed properties of geothermal water samples.

Parameters	Value	Cations	Concentration (mg/L)	Anions	Concentration (mg/L)
[a] pH	7.91 ± 0.66	[c]Li^+	1.18 ± 0.01	[b]HCO_3^-	583.15 ± 43.49
[a]EC^e (mS/cm)	1.75 ± 0.16	[c]Na^+	569.3 ± 259.79	[c]F^-	8.26 ± 2.74
[a] TDS^f (g/L)	0.88 ± 0.09	[c]K^+	36.2 ± 10.61	[c]Cl^-	311 ± 31.11
[a]Salinity (‰)	0.89 ± 0.09	[c]NH_4^+	22.06 ± 26.80	[c]NO_3^-	0.735 ± 1.04
[d]B (mg/L)	10.22 ± 0.03	[c]Ca^{2+}	16.39 ± 11.90	[c]SO_4^{2-}	191.15 ± 60.60
		[c]Mg^{2+}	24.08 ± 9.02		

[a] Hachlange HQ14D model multimeter; [b]Titrimetric method
[c]Shimadzu model ion chromatography (Prominence HIC-SP model);
[d]Spectrophotometric method (Shimadzu UV-1800 uv/vis spectrophotometer);
[e]Electrical conductivity; [f]Total Dissolved Solid.

Table 4. Specifications of ultrafiltration membrane module ZeeWeed®-1 (ZW-1, GE).

Specifications	Unit	
Effective membrane surface area	m^2	0.047
Nominal pore diameter	μm	0.04
Maximum permeation pressure	bar	0.6
Operating trans-membrane pressure	bar	0.07–0.55
Permeate flow range	mL/min	5–25
Membrane permeability range	L/m^2h	6.38–31.91
Maximum scouring air flow	m^3/h	1.8

Methods

The flow chart of the hybrid process was shown in Figure 1. The hybrid method couples the supply of fresh adsorbent suspension into the stirred suspension vessel in which a hollow-fiber-type UF membrane module was submerged. The adsorbents saturated with lithium ions were removed from the vessel were with the same rate of delivery of fresh adsorbents in a continuous mode of operation. The submerged hollow-fiber-type UF membrane module was employed for filtration of the adsorbent and to collect the permeate stream. Since geothermal water samples may contain the fine suspended particles which can cause clogging in UF process, a pre-treatment with microfiltration (MF) using 0.45-μm membrane filter prior to hybrid tests was applied. Initially, the volume of geothermal water in the vessel with UF module is 1.5 L. The concentrations of adsorbent in the vessel with submerged module and in the fresh adsorbent suspension were 1.0, 1.5, and 2.0 g/L. The feed flow rate into the stirred vessel with UF module and the rate of the permeate collection (Q_p) were adjusted as the same (as 5.0 and 10.0 mL/min, separately) to keep the volume of stirred vessel constant. On the other hand, the effect of adsorbent replacement speed (Q_s) was investigated with 3.0 and 6.0 mL/min of flow rates separately. A compressor was also employed for preventing accumulation of the adsorbents on the surface of the UF membrane by applying an air flow through the UF membrane module. The flow rate of air was kept constant as 4 L/min for all tests carried out. The permeate samples were taken at regular time intervals within 3 h (after 5, 10, 15, 20, 25, 30, 40, 60, 80, 100, 120, 140, 160, and 180 min). Due to the transfer of the fresh adsorbent suspension into the stirred suspension vessel via pure water, blank studies with only geothermal water in the suspension vessel and using only pure water in the fresh adsorbent tank (without addition of adsorbent) were performed for all of the parameters studied in order to determine the dilution effect on the lithium concentration of the geothermal water in the stirred suspension vessel.

Lithium contents of samples were determined by using an atomic absorption spectrophotometer (AAS, Shimadzu AA7000, Kyoto, Japan).
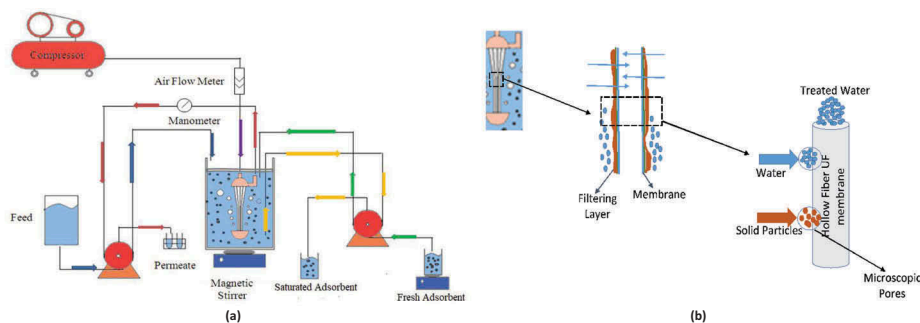
Figure 1. (a) The experimental set-up of the adsorption-membrane filtration hybrid system. (b) Cross-sectional view of hollow-fiber UF membrane.

Results and discussion

As a preliminary work, the efficiency of the ion exchange–membrane hybrid process was first tested for boron removal from aqueous solution. Commercially available chelating ion exchange resins containing *N*-methyl-*D*-glucamine groups were used as adsorbents, while MF membranes in hollow-fiber form were employed for filtration during hybrid process.[24,25] Güler et al.[27] studied the possibility of implementing a new hybrid system that integrates a reverse-osmosis (RO) process with an ion exchange–membrane filtration method for boron removal from seawater. It was found that the boron concentration in the product water did not fluctuate during 24 h of operation during sorption–membrane hybrid process.[27] In addition, Kabay et al.[30] investigated the recycle performance of the sorption–membrane hybrid system for boron removal from geothermal water by successive 10 sorption–washing–elution–washing–regeneration–washing cycles.

Taking into account the promising results for boron removal reported well in the literature, the similar process parameters such as adsorbent concentration, fresh and saturated adsorbents replacement rates, and permeate flow rate, along with adsorbent type were also investigated for separation of lithium from geothermal water by λ-MnO$_2$ adsorbent applying ion exchange–membrane filtration hybrid method. This adsorbent was developed and widely studied in Japan for lithium recovery from saline waters, and pilot-scale processes were evaluated by only the adsorption process.[6,7,9,10,13,17]

Effect of adsorbent type

Figure 2 shows the comparison of efficiencies for lithium separation from the geothermal water versus time in terms of the adsorbent concentration, permeate flow rate, and adsorbent replacement speed as 1.0 g/L, 5.0 mL/min, and 6.0 mL/min, respectively. Although the granulated adsorbent was usually preferred in column operations[6,7,9,17] to prevent the high-pressure drop occurred with powdery adsorbent, a faster separation of lithium with the powdery λ-MnO$_2$ adsorbent was obtained during an ion exchange–membrane filtration process. This was due to the increase in the effective surface area with decreasing particle size of the adsorbents as well as the binder in the granulated one, which greatly limited the access of lithium ions to the active adsorption sites. It was considered that the difference in adsorption capacities of both forms resulted in such behavior during hybrid process. For further studies, such operational parameters as adsorbent concentration, permeate flow rate, and adsorbent replacement speed were evaluated using powdery λ-MnO$_2$ adsorbent.
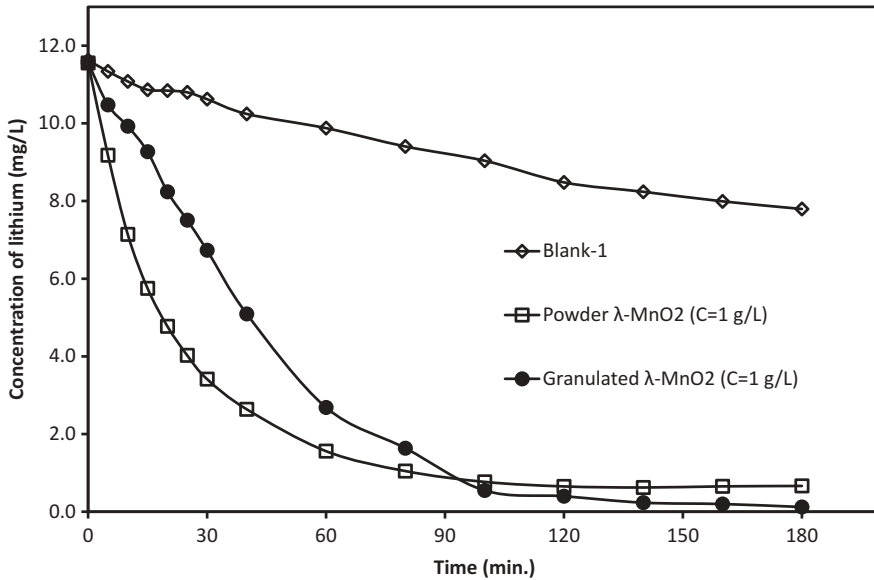
Figure 2. Effect of adsorbent form on lithium separation (C, g λ-MnO$_2$/L).

Effect of adsorbent dosage

Plots of lithium separation versus time are shown in Figures 3 and 4 for the adsorbent concentrations of 1.0, 1.5, and 2.0 g/L. The obtained data indicated that an increase in the adsorbent dosage resulted in a better efficiency for lithium separation. For the operational conditions either with 5.0 mL/min (Figure 3) or 10.0 mL/min (Figure 4) as the flow rates of the permeate stream and using 1.0 g/L of adsorbent concentration, lithium separation could not be effectively achieved. Thus, the increase of adsorbent concentration in the suspension seems to be needed for effective lithium separation from geothermal water.

Effect of permeate flow rate (Q_P)

Figure 5 shows the variation in lithium concentration in permeate sample at different permeate flow rates. When the flow rate of permeate was increased from 5.0 mL/min to 10.0 mL/min, the contact time with adsorbent decreased, and thus a higher concentration of lithium in permeate was observed. In the case of 5.0 mL/min of permeate flow rate, the lithium concentration in permeate was lowered to 0.62 mg/L after 140 min. However, in the case of 10 mL/min of permeate flow rate, the lowest lithium concentration in permeate was 2.39 mg/L after 60 min, and then it gradually increased to 3.65 mg/L after 3 h. This phenomenon was actually governed by the rate of replacement of suspension. It seems that at higher permeate flow rate, enough contact time might not be provided for lithium ions in the solution to reach active binding sites on the adsorbent. Similarly, the system was run with different adsorbent concentrations and replacement speeds to reveal the importance of contact time on adsorption process.

The effect of the permeate flow rate on lithium separation was also investigated with higher adsorbent concentration (2.0 g/L) and the rate of adsorbent replacement of 6.0 mL/min. The results are shown in Figure 6. Under permeate flow rate of 5.0 mL/min, a 100% of lithium separation was achieved after 60 min, while under permeate flow rate of 10 mL/min, the lowest lithium concentration in permeate was 0.06 mg/L after 80 min, and then it increased to 1.09 mg/L after 180 min.

Furthermore, the effect of the permeate flow rate on the lithium separation was investigated for the adsorbent concentration of 1.0 g/L when the adsorbent replacement rate was 3.0 mL/min. As
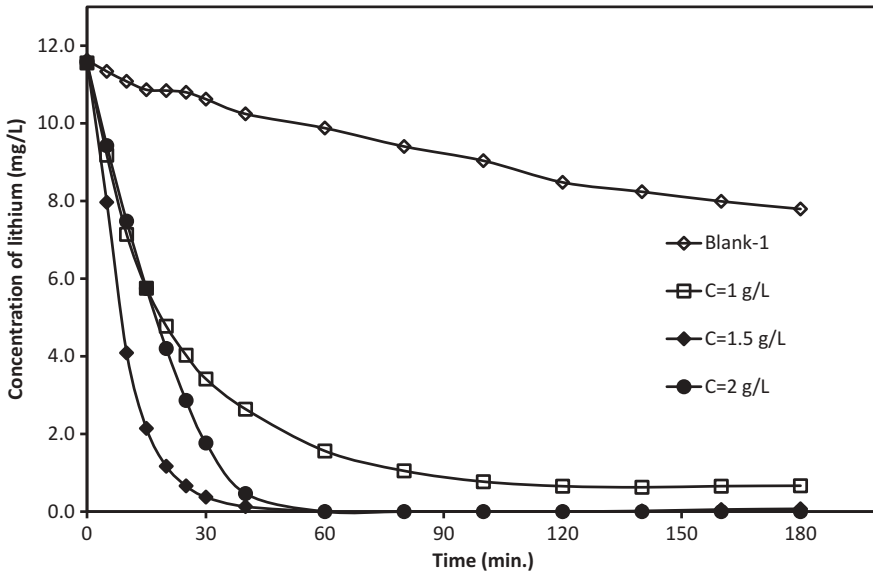
Figure 3. Effect of adsorbent concentration (*C*, g λ-MnO$_2$/L) on lithium separation. (*Q*s = 6.0 mL/min; *Q*p = 5.0 mL/min).
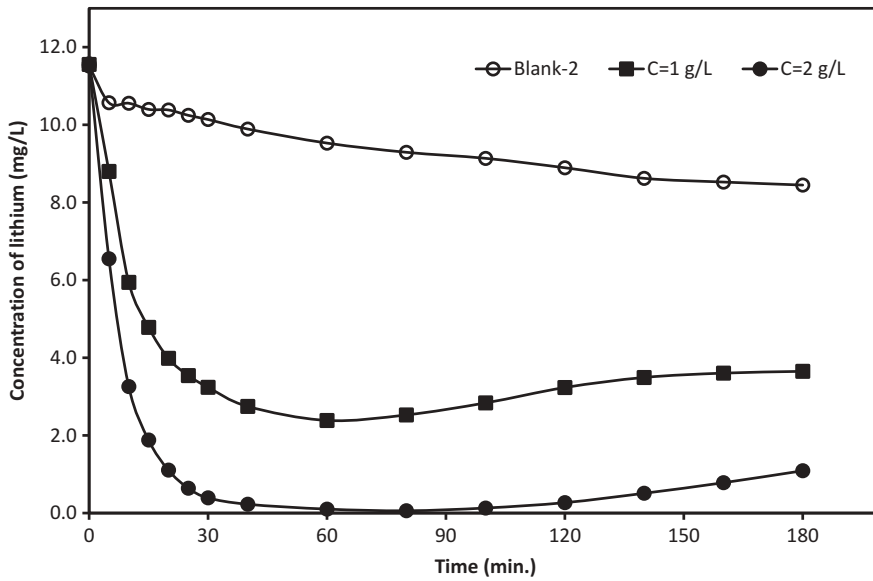

Figure 4. Effect of adsorbent concentration (*C*, g λ-MnO$_2$/L), on lithium separation. (*Q*s = 6.0 mL/min; *Q*p = 10.0 mL/min).

shown in Figure 7, when a slower rate of adsorbent replacement was applied, a lower efficiency for lithium separation was obtained in spite of the change in the permeate flow rate.
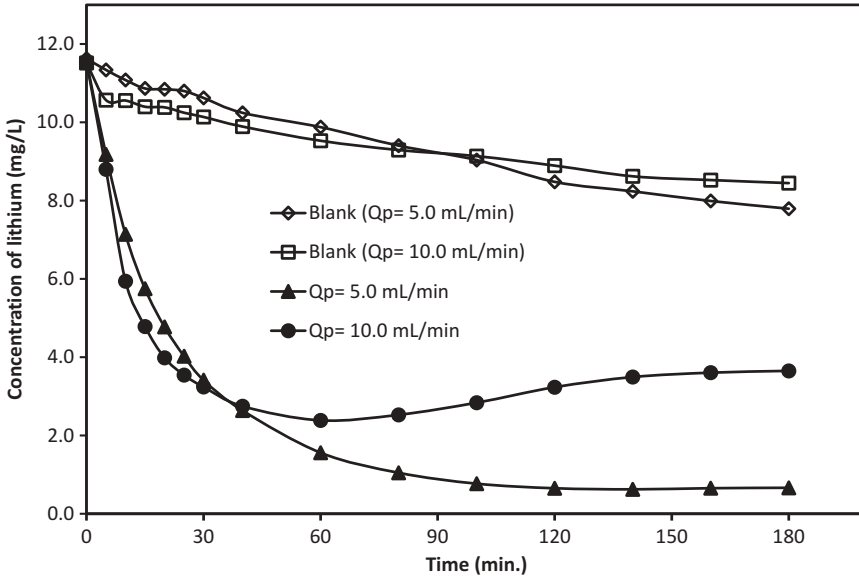
Figure 5. Effect of permeate flow rate on lithium separation.
($C = 1.0$ g λ-MnO$_2$/L; Qs $= 6.0$ mL/min).
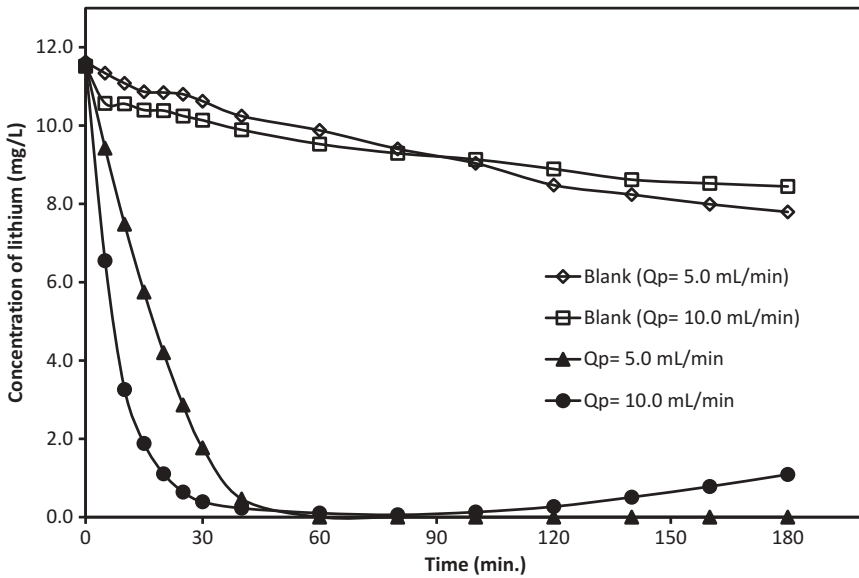
Figure 6. Effect of permeate flow rate on lithium separation.
($C = 2.0$ g λ-MnO$_2$/L; Qs $= 6.0$ mL/min).

Effect of adsorbent replacement speed (Q_s)

Figure 8 shows the lithium concentrations in permeates for two different rates of adsorbent replacements, 3.0 and 6.0 mL/min, with a permeate flow rate of 5.0 mL/min. As the adsorbent replacement rate was increased moderately, a better lithium separation was achieved due to the increase in favorable active sites by the continuous addition of fresh adsorbent to the system to
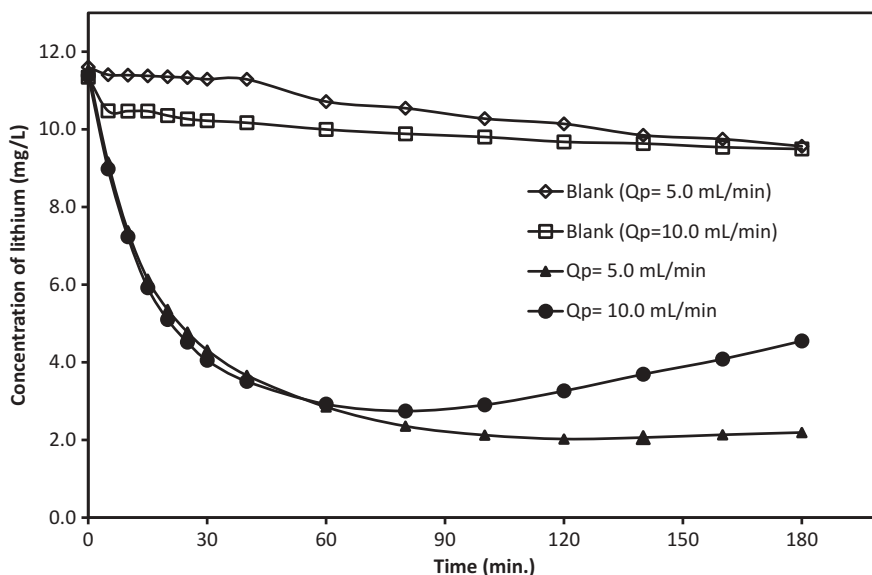
Figure 7. Effect of permeate flow rate on lithium separation.
(C = 1.0 g MnO_2/L; Qs = 3.0 mL/min).

contact with lithium ions in the solution and the removal of saturated adsorbent from the system at the same speed.

In the case of the adsorbent replacement rate of 6.0 mL/min, lithium concentration in permeate was lowered to 0.62 mg/L after 140 min. However, in the case of adsorbent replacement rate of 3.0 mL/min, the lowest lithium concentration in the permeate was 2.02 mg/L after 120 min, and then it gradually increased to 2.19 mg/L after 3 h of operation.

Figure 9 shows the effect of the adsorbent replacement rate on the lithium separation under a higher permeate flow rate of 10 mL/min. Compared with the lower permeate flow rate, an increase in the rate of adsorbent replacement yielded a more effective lithium separation.

The obtained kinetic data were also analyzed using four kinetic models: the pseudo-first-order, pseudo-second-order, Elovich, and intraparticle diffusion models.

The pseudo-first-order kinetic model[34] is defined in (Equation 2):

$$\ln(q_e - q_t) = \ln q_e - k_1 t \tag{2}$$

where q_e and q_t (mg/g) are the adsorption amounts at equilibrium and at time, t (min), respectively, and k_1 (min^{-1}) is the adsorption rate constant. The values of k_1 and q_e were calculated from slope and the intercept of the plot of $\ln(q_e - q_t)$ versus t, respectively.

The pseudo-second-order equation[34] based on equilibrium adsorption is expressed in (Equation 3):

$$\frac{t}{q_t} = \frac{1}{k_2 q_e^2} + \frac{1}{q_e} t \tag{3}$$

where k_2 (g/mg min) is the rate constant of second-order adsorption, while q_e and k_2 were calculated from the slope and intercept of the plot of t/q_t versus t, respectively.

The Elovich equation is one of the most useful models for describing activated chemisorption. After arrangement and simplification, the Elovich equation[34] can be expressed as in (Equation 4):
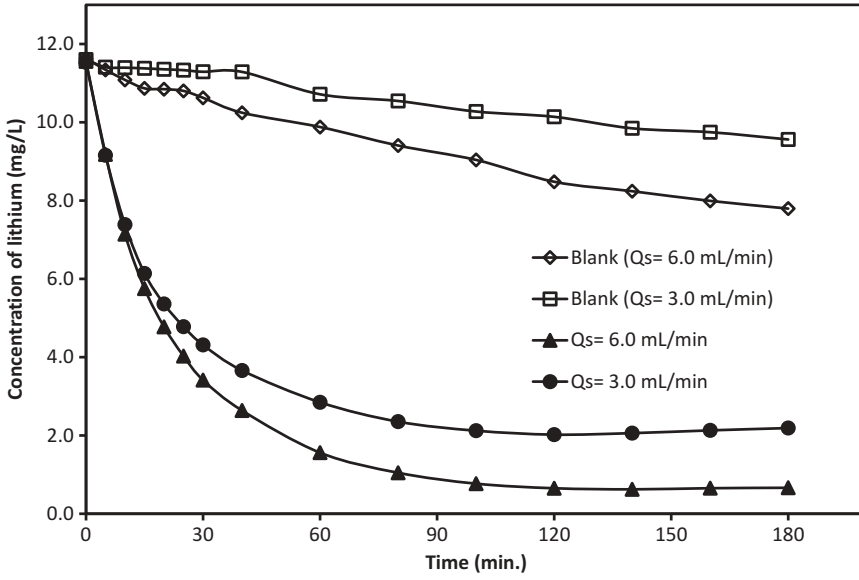
Figure 8. Effect of adsorbent replacement rate on lithium separation.
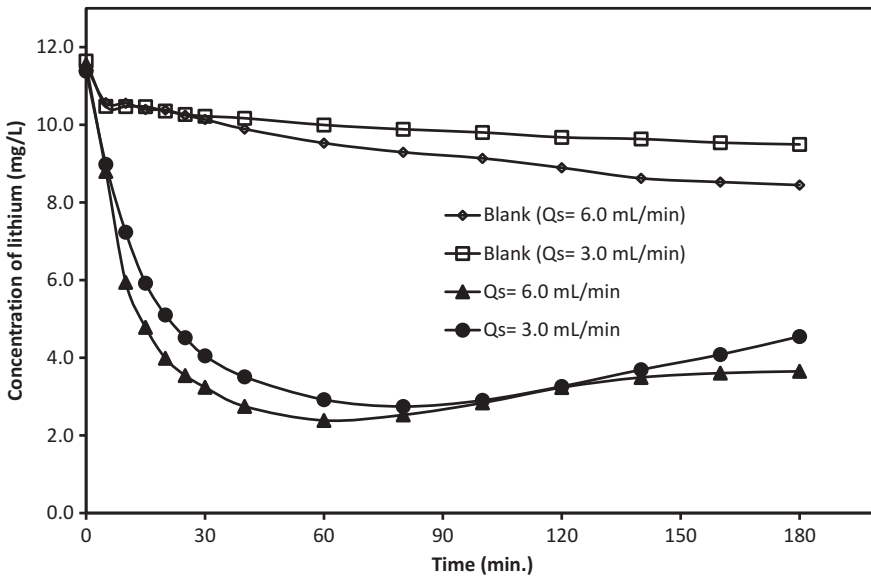(C = 1.0 g MnO_2/L; Qp = 5.0 mL/min).

Figure 9. Effect of adsorbent replacement rate on lithium separation.
(C = 1.0 g MnO_2/L; Qp = 10.0 mL/min).

$$q_t = \left(\frac{1}{\beta}\right) \ln(\alpha\beta) + \left(\frac{1}{\beta}\right) \ln t \qquad (4)$$

where α and β are the constants for this model obtained from the slope and intercept of the linear plot of q_t versus $\ln t$.

As the above kinetic models are not able to identify the diffusion mechanism, intraparticle diffusion model is an empirically found functional relationship based on the theory proposed by Weber and Morris[34] as follows in (Equation 5):

$$q_t = k_i t^{1/2} + C_i \tag{5}$$

where C_i [mg g^{-1}] refers to the equilibrium capacity and k_i [mg g^{-1} min$^{1/2}$] is the intraparticle diffusion rate constant. C_i and k_i can be calculated from the intercept and slope of the linear plot of q_t versus $t^{1/2}$, respectively.

The values of kinetic parameters obtained with adsorbent dosage of C = 1.5 g/L for powdery λ-MnO$_2$ adsorbent were tabulated in Table 5. The linearity of the plots with relatively higher R^2 values obtained using pseudo-first-order kinetic model proved the applicability of pseudo-first-order kinetic model for the kinetic data obtained. When compared the experimental adsorption capacity (q_e) with the calculated adsorption capacity ($q_{calc.}$) values given in Table 5, for each model, the mechanism of lithium adsorption can be explained well by the pseudo-first-order kinetic model. That is, the rate is determined by pore diffusion clarifying by the hole formed in the adsorbent after acid treatment. In our previous batch equilibrium and kinetic studies,[22] the rate constant has been found as 0.053 min^{-1}. However, in this study, it is found to be 0.120 min^{-1}, and this result confirms the system intensification with better kinetics and high efficiency.

Conclusions

In this study, a hybrid process coupling ion exchange with UF was suggested for lithium separation from geothermal water as an alternative method to conventional fixed-bed operation requiring longer operation time. The hybrid system is considered to be a cost-effective process for applying powdery λ-MnO$_2$ adsorbent to lithium separation from geothermal water. The effects of the process parameters such as physical form of the adsorbent (granulated or powdery forms), adsorbent concentration, flow rates of feed/permeate streams, and replacement rates of saturated and fresh adsorbents on the efficiency of lithium separation from geothermal water were investigated. The obtained results are summarized in Table 6. The optimal operating conditions were 1.5 g/L of the adsorbent concentration, 5.0 mL/min of the feed/permeate flow rate, and 6.0 mL/min of the replacement rate of fresh/saturated adsorbents. It was concluded that the lithium separation can be achieved more efficiently by increasing the replacement rate of saturated and fresh adsorbent as well as by decreasing the flow rate of permeate.

For further investigation, as recommended in our previous work, regeneration of lithium selective adsorbents could be done using an acid solution (e.g., 1 M HCl) following sorption step of ion exchange–membrane filtration hybrid method.[33] The bipolar membrane electrodialysis method could be considered for recovering lithium from the regenerant solution in the following step.[35,36]

Table 5. Pseudo-first-order model, pseudo-second-order model, Elovich model, and Intraparticle diffusion model constants and correlation coefficients for adsorption of lithium on powder λ-MnO$_2$ adsorbent (C = 1.5g/L; Qp = 5.0mL/min; Qs = 6.0mL/min)^a.

		Pseudo-first order kinetic model			Pseudo-second order kinetic model			Elovich model			Intra-particle diffusion model		
Adsorbent Type	$q_{e,exp.}$ (mg/ g)	$q_{e,calc.}$ (mg/ g)	k_1 (min^{-1})	R^2	$q_{e,calc.}$ (mg/ g)	k_2 (g/mg min)	R^2	β	α	R^2	k_i (mg/g min$^{1/2}$)	C_i (mg/ g)	R^2
Powdery λ-MnO$_2$	9.6	10.97	0.12	1.00	13.05	0.0063	0.96	0.312	2.039	0.94	0.94	1.54	0.84

^{a}C: adsorbent concentration in the suspension; Qp: permeate flow rate; Qs: adsorbent replacement speed.

Table 6. Evaluation of results obtained from adsorption-membrane filtration hybrid system.

Test no.	C (g/L)	Q_s (mL/min)	Q_p (mL/min)	$[Li]_0$ (mg/L)	$[Li]_1$ (mg/L)	$[Li]_2$ (mg/L)
1	0.0	6.0	5.0	11.63	7.79	7.79
2	0.0	6.0	10.0	11.51	8.45	8.45
3	0.0	3.0	5.0	11.60	9.56	9.56
4	0.0	3.0	10.0	11.34	9.49	9.49
5[a]	1.0	6.0	5.0	11.57	0.12	0.12
6	1.0	6.0	5.0	11.55	0.62	0.66
7	2.0	6.0	5.0	11.57	0.00	0.00
8	1.0	3.0	5.0	11.53	2.02	2.19
9	1.0	6.0	10.0	11.56	2.39	3.65
10	2.0	6.0	10.0	11.57	0.06	1.09
11	1.5	6.0	5.0	11.58	0.00	0.07
12	1.0	3.0	10.0	11.38	2.74	4.55

$[Li]_0$: initial Li concentration; $[Li]_1$: the first lowest Li concentration in permeate; $[Li]_2$: Li concentration in permeate at the end of process; C: adsorbent concentration in the suspension; Q_s: adsorbent replacement speed; Q_p: permeate flow rate.
[a]Data belong to granulated type adsorbent.

Acknowledgments

Funding

References

[1] Swain, B.;. Recovery and Recycling of Lithium: A Review. *Sep. Purif. Technol.* 2017, *172*, 388–403. DOI: 10.1016/j.seppur.2016.08.031.

[2] Cao, J.; Shi, J.; Hu, Y.; Wu, M.; Ouyang, C.; Xu, B. Lithium Ion Adsorption and Diffusion on Black Phosphorene Nanotube: A First-Principles Study. *Appl. Surf. Sci.* 2017, *392*, 88–94. DOI: 10.1016/j.apsusc.2016.09.004.

[3] Xu, X.; Chen, Y.; Wan, P.; Gasem, K.; Wang, K.; He, T.; Adidharma, H.; Fan, M. Extraction of Lithium with Functionalized Lithium Ion-Sieves. *Prog. Mater. Sci.* 2016, *84*, 276–313. DOI: 10.1016/j.pmatsci.2016.09.004.

[4] Singh, M.; Kaiser, J.; Hahn, H. A Systematic Study of Thick Electrodes for High Energy Lithium Ion Batteries. *J. Electroanal. Chem.* 2016, *782*, 245–249. DOI: 10.1016/j.jelechem.2016.10.040.

[5] Shi, C.; Jing, Y.; Xiao, J.; Wang, X.; Yao, Y.; Jia, Y. Solvent Extraction of Lithium from Aqueous Solution Using Non-Fluorinated Functionalized Ionic Liquids as Extraction Agents. *Sep. Purif. Technol.* 2017, *172*, 473–479. DOI: 10.1016/j.seppur.2016.08.034.

[6] Park, J.; Sato, H.; Nishihama, S.; Yoshizuka, K. Lithium Recovery from Geothermal Water by Combined Adsorption Methods. *Solvent Extr.Ion Exchange.* 2012, *30*, 398–404. DOI: 10.1080/07366299.2012.687165.

[7] Park, J.; Sato, H.; Nishihama, S.; Yoshizuka, K. Separation and Recovery of Lithium from Geothermal Water by Sequential Adsorption Process with λ –Mno$_2$ and TiO$_2$. *Ion Exchange Lett.* 2012, *5*, 1–5.

[8] Zandevakili, S.; Ranjbar, M.; Ehteshamzadeh, M. Recovery of Lithium from Urmia Lake by a Nanostructure MnO$_2$ Ion Sieve. *Hydrometallurgy.* 2014, *149*, 148–152. DOI: 10.1016/j.hydromet.2014.08.004.

[9] Kitajou, A.; Suzuki, T.; Nishihama, S.; Yoshizuka, K. Selective Recovery of Lithium from Seawater Using a Novel MnO$_2$ Type Adsorbent II – Enhancement of Lithium Ion Selectivity of the Adsorbent. *Ars Separatoria Acta.* 2003, *2*, 97–106.

[10] Kitajou, A.; Holba, M.; Suzuki, T.; Nishihama, S.; Yoshizuka, K. Selective Recovery System of Lithium from Seawater Using a Novel Granulated λ-MnO$_2$ Adsorbent. *J. Ion Exchange.* 2005, *16*, 49–54. DOI: 10.5182/jaie.16.49.

[11] Iizuka, A.; Yamashita, Y.; Nagsawa, H.; Yamasaki, A.; Yanagisawa, Y. Separation of Lithium and Cobalt from Waste Lithium-Ion Batteries via Bipolar Membrane Electrodialysis Coupled with Chelation. *Sep. Purif. Technol.* 2013, *113*, 33–41. DOI: 10.1016/j.seppur.2013.04.014.

[12] Somrani, A.; Hamzaoui, A. H.; Pontie, M. Study on Lithium Separation from Salt Lake Brines by Nanofiltration (NF) and Low Pressure Reverse Osmosis (LPRO). *Desalination*. 2013, *317*, 184–192. DOI: 10.1016/j.desal.2013.03.009.

[13] Yoshizuka, K.; Fukui, K.; Inoue, K. Selective Recovery of Lithium from Seawater Using a Novel MnO_2 Type Adsorbent. *Ars Separatoria Acta*. 2002, *1*, 79–86.

[14] Chitrakar, R.; Kanoh, H.; Miyai, Y.; Ooi, K. Synthesis of o-$LiMnO_2$ by Microwave Irradiation and Study Its Heat Treatment and Lithium Exchange. *J. Solid State Chem*. 2002, *163*, 1–4. DOI: 10.1006/jssc.2001.9403.

[15] Chitrakar, R.; Kasaishi, S.; Umeno, A.; Sakane, K.; Takagi, N.; Kim, Y.; Ooi, K. Synthesis and Characterization of Lithium Nickel Manganese Oxides and Their Delithiated Phases. *J. Solid State Chem*. 2002, *169*, 35–43. DOI: 10.1016/S0022-4596(02)00014-2.

[16] Kim, Y.; No, K.; Chung, K.; Lee, J.; Ooi, K. Li^+ Extraction Reactions with Spinel-Type $LiM_{0.5}Mn_{1.5}O_4$ (M=Ti, Fe) and Their Electronic Structures. *Mater. Lett*. 2003, *57*, 4140–4146. DOI: 10.1016/S0167-577X(03)00279-9.

[17] Nishihama, S.; Onishi, K.; Yoshizuka, K. Selective Recovery Process of Lithium from Seawater Using Integrated Ion Exchange Methods. *Solvent Extr.Ion Exchange*. 2011, *29*, 421–431. DOI: 10.1080/07366299.2011.573435.

[18] Yu, Q.; Sasaki, K.; Hirajima, T. Bio-Templated Synthesis of Lithium Manganese Oxide Microtubes and Their Application in Li^+ Recovery. *J. Hazard. Mater*. 2013, *262*, 38–47. DOI: 10.1016/j.jhazmat.2013.08.027.

[19] Li, L.; Qu, W.; Liu, F.; Zhao, T.; Zhang, X.; Chen, R.; Wu, F. Surface Modification of Spinel λ –Mno_2 and Its Lithium Adsorption Properties from Spent Lithium Ion Batteries. *Appl. Surf. Sci*. 2014, *315*, 59–65. DOI: 10.1016/j.apsusc.2014.07.090.

[20] Noerochim, L.; Satriawangsa, G. A.; Susanti, D.; Widodo, A. Synthesis and Characterization of Lithium Manganese Oxide with Different Ratio of Mole on Lithium Recovery Process from Geothermal Fluid of Lumpur Sidoarjo. *J. Mater. Sci. Chem. Eng*. 2015, *3*, 56–62. DOI: 10.4236/msce.2015.311007.

[21] Li, L.; Deshmane, V.; Paranthaman, M. P.; Bhave, R.; Moyer, B.; Harrison, S. Lithium Recovery from Aqueous Resources and Batteries: A Brief Review. *Johnson Matthey Technol. Rev*. 2018, *62*(2), 161–176. DOI: 10.1595/205651317X696676.

[22] Recepoğlu, Y. K.; Kabay, N.; Yılmaz-İpek, İ.; Arda, M.; Yoshizuka, K.; Nishihama, S.; Yüksel, M. Equilibrium and Kinetic Studies on Lithium Adsorption from Geothermal Water by λ-MnO_2. *Solvent Extr.Ion Exchange*. 2017, *35*, 221–231. DOI: 10.1080/07366299.2017.1319235.

[23] Koltuniewicz, A. B.; Witek, A.; Bezak, K. Efficiency of Membrane-Sorption Integrated Processes. *J. Memb. Sci*. 2004, *239*, 129–141. DOI: 10.1016/j.memsci.2004.02.037.

[24] Yılmaz, İ.; Kabay, N.; Bryjak, M.; Yüksel, M.; Wolska, J. A Submerged Membrane–Ion-Exchange Hybrid Process for Boron Removal. *Desalination*. 2006, *198*, 310–315. DOI: 10.1016/j.desal.2006.01.031.

[25] Kabay, N.; Yılmaz, İ.; Bryjak, M.; Yüksel, M. Removal of Boron from Aqueous Solutions by a Hybrid Ion Exchange–Membrane Process. *Desalination*. 2006, *198*, 158–165. DOI: 10.1016/j.desal.2006.09.011.

[26] Kabay, N.; İpek-Yılmaz, İ.; Soroko, I.; Makowski, M.; Kırmızısakal, O.; Yağ, S.; Bryjak, M.; Yüksel, M. Removal of Boron from Balcova Geothermal Water by Ion Exchange-Microfiltration Hybrid Process. *Desalination*. 2009, *241*, 167–173. DOI: 10.1016/j.desal.2007.10.100.

[27] Güler, E.; Kabay, N.; Yüksel, M.; Yiğit, N. Ö.; Kitiş, M.; Bryjak, M. Integrated Solution for Boron Removal from Seawater Using RO Process and Sorption-Membrane Filtration Hybrid Method. *J. Memb. Sci*. 2011, *375*, 249–257. DOI: 10.1016/j.memsci.2011.03.050.

[28] Yılmaz-İpek, İ.; Kabay, N.; Yüksel, M.; Yapıcı, D.; Yüksel, Ü. Application of Adsorption–Ultrafiltration Hybrid Method for Removal of Phenol from Water by Hypercrosslinked Polymer Adsorbents. *Desalination*. 2012, *306*, 24–28. DOI: 10.1016/j.desal.2012.08.033.

[29] Kabay, N.; Köseoğlu, P.; Yavuz, E.; Yüksel, Ü.; Yüksel, M. An Innovative Integrated System for Boron Removal from Geothermal Water Using RO Process and Ion Exchange-Ultrafiltration Hybrid Method. *Desalination*. 2013, *316*, 1–7. DOI: 10.1016/j.desal.2013.01.020.

[30] Kabay, N.; Köseoğlu, P.; Yapıcı, D.; Yüksel, Ü.; Yüksel, M. Coupling Ion Exchange with Ultrafiltration for Boron Removal from Geothermalwater-Investigation of Process Parameters and Recycle Tests. *Desalination*. 2013, *316*, 17–22. DOI: 10.1016/j.desal.2013.01.027.

[31] Samatya, S.; Köseoğlu, P.; Kabay, N.; Tuncel, A.; Yüksel, M. Utilization of Geothermal Water as Irrigation Water after Boron Removal by Monodisperse Nanoporous Polymers Containing NMDG in Sorption–Ultrafiltration Hybrid Process. *Desalination*. 2015, *364*, 62–67. DOI: 10.1016/j.desal.2015.02.030.

[32] Yılmaz-İpek, İ.; Yüksel, S.; Kabay, N.; Yüksel, M. Investigation of Process Parameters for Removal of Bisphenol A (BPA) from Water by Polymeric Adsorbents in Adsorption-Ultrafiltration Hybrid System. *J. Chem. Technol. Biotechnol*. 2014, *89*, 835–840. DOI: 10.1002/jctb.4317.

[33] Recepoğlu, Y. K.; Kabay, N.; Yılmaz-İpek, İ.; Arda, M.; Yüksel, M.; Yoshizuka, K.; Nishihama, S. Elimination of Boron and Lithium Coexisting in Geothermal Water by Adsorption-Membrane Filtration Hybrid Process. *Sep. Sci. Technol*. 2018, *53*, 856–862. DOI: 10.1080/01496395.2017.1405985.

[34] Hameed, B. H.; Tan, I. A. W.; Ahmad, A. L. Adsorption Isotherm, Kinetic Modeling and Mechanism of 2, 4, 6-Trichlorophenol on Coconut Husk-Based Activated Carbon. *Chem. Eng. J*. 2008, *144*, 235–244. DOI: 10.1016/j.cej.2008.01.028.

[35] Bunani, S.; Arda, M.; Kabay, N.; Yoshizuka, K.; Nishihama, S. Effect of Process Conditions on Recovery of Lithium and Boron from Water Using Bipolar Membrane Electrodialysis (BMED). *Desalination.* 2017, *416*, 10–15. DOI: 10.1016/j.desal.2017.04.017.

[36] Bunani, S.; Yoshizuka, K.; Nishihama, S.; Arda, M.; Kabay, N. Application of Bipolar Membrane Electrodialysis (BMED) for Simultaneous Separation and Recovery of Boron and Lithium from Aqueous Solutions. *Desalination.* 2017, *424*, 37–44. DOI: 10.1016/j.desal.2017.09.029.